

# Fracture toughness analysis of laser-beam-welded superalloys Inconel 718 and 625

C. YENI<sup>1</sup> and M. KOÇAK<sup>2</sup>

<sup>1</sup>Dokuz Eylül University, Faculty of Engineering, 35100 Bornova, Izmir, Turkey (currently at GKSS Research Center), <sup>2</sup>GKSS Research Center, Institute for Materials Research, D-21502, Geesthacht, Germany

Received in final form 31 January 2005

**ABSTRACT** In this study, two 3.2-mm thick Ni-base superalloys, Inconel 718 and 625, have been laser-beam-welded by a 6-kW CO<sub>2</sub> laser and their room temperature fracture toughness properties have been investigated. Fracture toughness behaviour of the base metal (BM), fusion zone (FZ) and heat affected zone (HAZ) regions was determined in terms of crack tip opening displacement (CTOD) using compact tension-type (C(T)) specimens. Laser-beam-weld regions showed no significant strength overmatching in both alloys. Ductile crack growth analysis (R-curve) also showed that both materials exhibited similar behaviour. Compared to the BM there is a slight decrease in fracture toughness of the fusion and the HAZ.

**Keywords** CTOD; fracture toughness; laser-beam welding; R-curve; superalloy.

## NOMENCLATURE

$a_0$  = initial crack length (mm)  
 $A$  = total elongation (%)  
 BM = base metal  
 C(T) = compact tension  
 CTOD = crack tip opening displacement  
 FZ = fusion zone  
 $F$  = load (kN)  
 $F_{\max}$  = maximum load (kN)  
 $H$  = half weld width (mm)  
 HAZ = heat affected zone  
 $L_0$  = initial gauge length in transverse tensile specimen (mm)  
 $L_{0\text{eff}}$  = effective gauge length ( $=L_0-2H$ )  
 $M$  = mis-match ratio ( $=R_{p0.2\text{WM}}/R_{p0.2\text{BM}}$ )  
 $R_{p0.2}$  = yield strength at 0.2% plastic strain (MPa)  
 R-curve = crack resistance curve  
 $R_m$  = ultimate tensile strength (MPa)  
 $W$  = width of C(T) specimen (mm)  
 WM = weld metal  
 $\delta_5$  = CTOD measured over a gauge length of 5 mm (mm)  
 $\delta_{5\max}$  =  $\delta_5$  measured at  $F_{\max}$  (mm)  
 $\Delta a$  = crack extension (mm)  
 $\Delta L$  = increase in  $L_0$  (mm)  
 $\varepsilon$  =  $\Delta L/L_0$

## INTRODUCTION

Alloy 718 of Ni-based superalloys is an age-hardenable, high-strength alloy suitable for service temperatures from

Correspondence: C. Yeni. E-mail: emine.cinar@deu.edu.tr

–250 to 705 °C. The fatigue strength of Inconel 718 is high and the alloy exhibits excellent stress-rupture properties up to 705 °C, as well as oxidation resistance up to 982 °C.<sup>1</sup> These unique properties have resulted in its use in a wide range of applications such as gas turbine components, cryogenic storage tanks, jet engines, pump bodies, rocket motors, thrust reversers, nuclear fuel element spacers, etc. Inconel 718 is reported to be resistant to strain-age cracking as a result of the sluggish precipitation kinetics of its principal strengthening precipitate  $\gamma''$  ( $\text{Ni}_3\text{Nb}$ ).<sup>2</sup> The alloy, however, is not totally free from weldability problems that include solidification cracking and microfissuring in the heat affected zone (HAZ).<sup>2</sup> In the fusion welding of Inconel 718, the solidification begins with the formation of Nb-lean austenitic dendrites. Non-equilibrium interdendritic eutectics, consisting of MC-type carbides and a Nb-rich Laves phase, form in these alloys at high temperature and solidification terminates with the  $\gamma$ /Laves eutectic.<sup>3</sup> It is a brittle, intermetallic compound represented as  $(\text{Ni}, \text{Cr}, \text{Fe})_2(\text{Nb}, \text{Mo}, \text{Ti})$  in the interdendritic regions during weld metal solidification. It has been demonstrated that Laves phase is detrimental to weld metal mechanical properties, particularly with respect to ductility, fracture toughness, fatigue and creep rupture properties as it aids in easy crack initiation and propagation, in addition to consuming significant amounts of useful alloying elements.<sup>4–7</sup>

Laser welding, due to its inherently narrow HAZ, offers potential promise for producing crack-free joints in Inconel 718.<sup>8</sup> Welding studies of Inconel 718 on joints made with a 15-kW continuous wave (CW)  $\text{CO}_2$  laser indicated that it could be an effective joining method for up to 12 mm thickness.<sup>2</sup> A pronounced ‘nailhead’ geometry was produced and microcracks and some porosity were observed in the literature.<sup>9</sup> Pulsed Nd:YAG laser welding and electron-beam welding studies conducted on this material have shown that the material cracked in the nailhead weld metal.<sup>10</sup> The weld metal cracks were attributed to hot cracking under the nailhead due to the thermal stresses and the solidification temperature interval.<sup>10</sup> Investigation of the various aspects of CW and pulsed laser welding of wrought and cast Inconel 718 showed that, through appropriate control of the welding parameters, specifically the heat source with pulse tailoring and plasma location

manipulation, the weld shape and thermal history could be varied. These studies indicated that while laser welding may suffer from nailhead cracking, it does offer the possibility of controlling the HAZ cracking problems.<sup>9</sup>

The second material of this study, Inconel 625 is a solid-solution matrix-stiffened face-centred cubic alloy. It may contain carbides, in the form of MC and  $\text{M}_6\text{C}$  (rich in Ni, Nb, Mo and C), which are inherent in this type of alloy. The hardening effect that takes place in the material on exposure in the range centred around 649 °C, is due to sluggish precipitation of a Ni–Nb rich  $\gamma'$  phase.<sup>4</sup> Nickel–chromium alloy 625 is used for its good high-temperature strength, excellent fabricability including joining and corrosion resistance. Service temperatures range from cryogenic to 982 °C. High weldability properties of Inconel 625 make it interesting to the aerospace field. It is being used in applications such as aircraft ventilation systems, engine exhaust systems, thrust reversers, etc. Unlike precipitation hardened superalloys, the Al (0.40% max.) and Ti (0.40% max.) contents in this alloy are limited, which eliminates strain-age cracking problem. The addition of Nb, however, promotes HAZ liquation (also called microfissuring), although this alloy is normally considered to have good weldability.<sup>9</sup> Recent studies<sup>11–13</sup> have indicated that this alloy can be susceptible to microfissuring. Çam *et al.*<sup>11</sup> have investigated in the framework of EU project ASPOW,<sup>14</sup> the 2 kW Nd:YAG laser welding of both Inconels 718 and 625 in 3-mm-thick materials with a welding speed of 0.5 m/min under argon and these were crack-free welds.

A survey on the literature review of Inconels 718 and 625 has indicated that more data are needed on the weld mechanical properties, especially when welded using advanced welding techniques such as laser-beam welding, of these alloys. Some suggested data on this subject are given in Refs [15] and [16]. This requirement, together with a lack of information on the fracture toughness properties of  $\text{CO}_2$  laser-beam-welded Inconels 718 and 625 alloys in thin plate forms, has led to the present study to determine the tensile and fracture toughness properties and use this data for structural integrity assessment of flaws in such welded structural components made of superalloys. However, this paper reports only the fracture toughness properties of both alloys.

**Table 1** Chemical compositions of Inconels 718 and 625 alloys (in wt%)

Material	C	Mn	Fe	S	Cu	Ni	Cr	Al	Ti	Co	Mo	Nb	Ta	P	Si	B	N
Inconel 718	0.03	0.08	16.1	0.0001	0.07	53.70	18.39	0.49	1.00	0.14	2.96	4.92	0.01	0.011	0.10	0.003	–
Inconel 625	0.01	0.06	4.53	<0.001	–	60.55	21.72	0.19	0.28	0.19	8.90	3.47	0.01	0.005	0.07	–	0.014

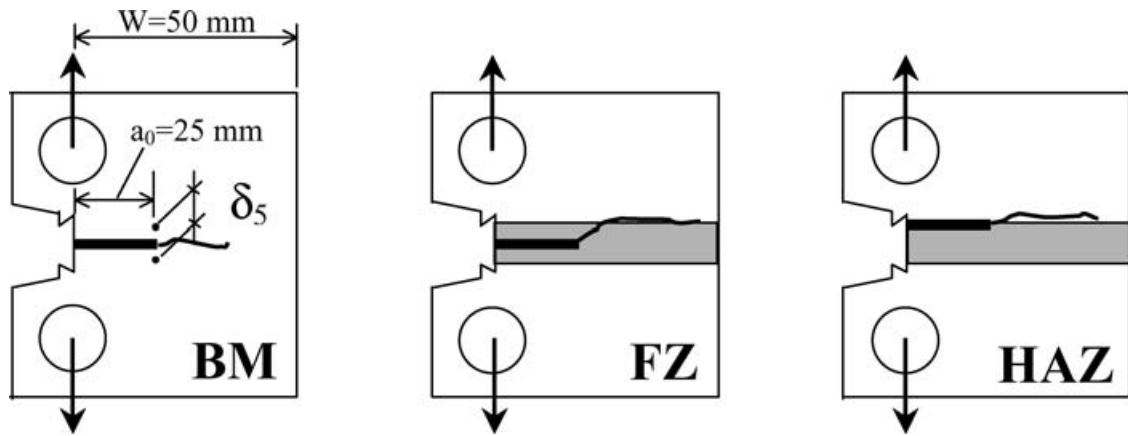


Fig. 1 C(T) specimen configurations used for fracture toughness tests ( $W = 50 \text{ mm}$ ,  $a/W = 0.5$ ).

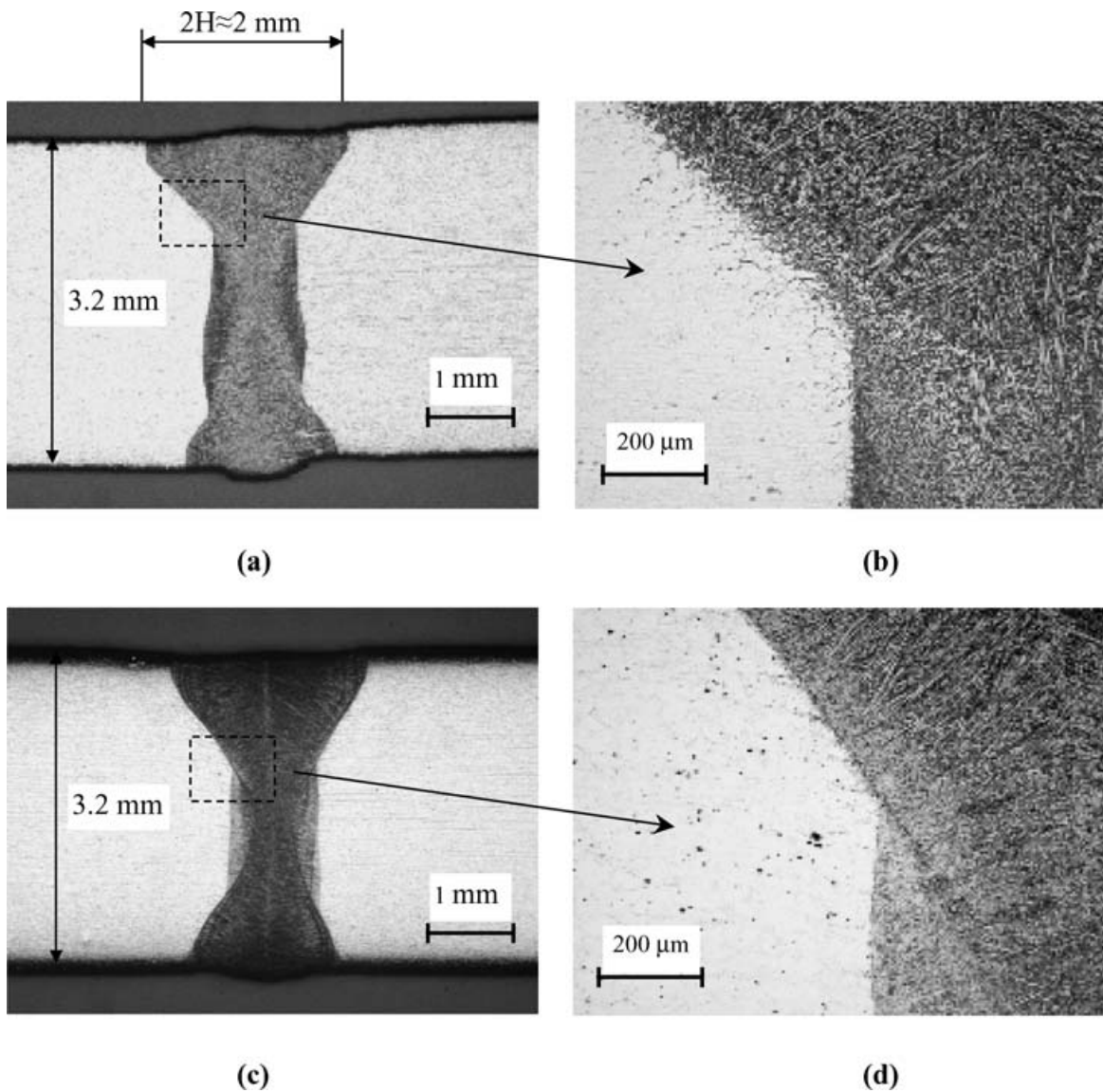


Fig. 2 (a) Cross section of the weld, Inconel 718 and (b) higher magnification micrograph of its joint area, (c) cross section of the weld, Inconel 625 and (d) higher magnification micrograph of its joint area.

## MATERIALS AND EXPERIMENTAL PROCEDURE

Materials used in this study were Inconels 718 and 625 thin plates with a thickness of 3.2 mm. Autogenous laser-beam welds (butt-joints) have been produced in these alloys using a CW 6 kW CO<sub>2</sub> laser within the framework of the EU project ASPOW. Welding parameters have been adjusted in order to get the optimum weld bead shape and to prevent microfissuring. The welds were used in as-welded condition without the application of any heat treatments. Crack-free welds have been achieved for both types of alloys. The chemical compositions of the alloys are given in Table 1.

The as-welded samples were characterized for their microstructural aspects using scanning electron microscopy (SEM). Room temperature tensile properties of the base

and the weld metals are determined by the use of flat transverse tensile specimens with a gauge length of 40 mm. In welded specimens, the welds were transverse to the loading direction. ASTM E 8-95a test method has been employed in the tensile tests.<sup>17</sup> Microhardness measurements (using a 200 g load) across the weld joints have been carried out to establish the hardness variations. In order to determine the crack tip opening displacement (CTOD) fracture toughness in terms of crack resistance curves (R-Curves) of the base metal (BM), FZ and HAZ regions, standard fracture toughness tests of compact tension (C(T)) specimens ( $W = 50$  mm,  $B = 3.2$  mm,  $a/W = 0.5$ ) have been conducted at room temperature. The CTOD values were measured directly using  $\delta_5$  clip-on-gauges at the fatigue crack tip over a gauge length of 5 mm, as shown in Fig. 1.

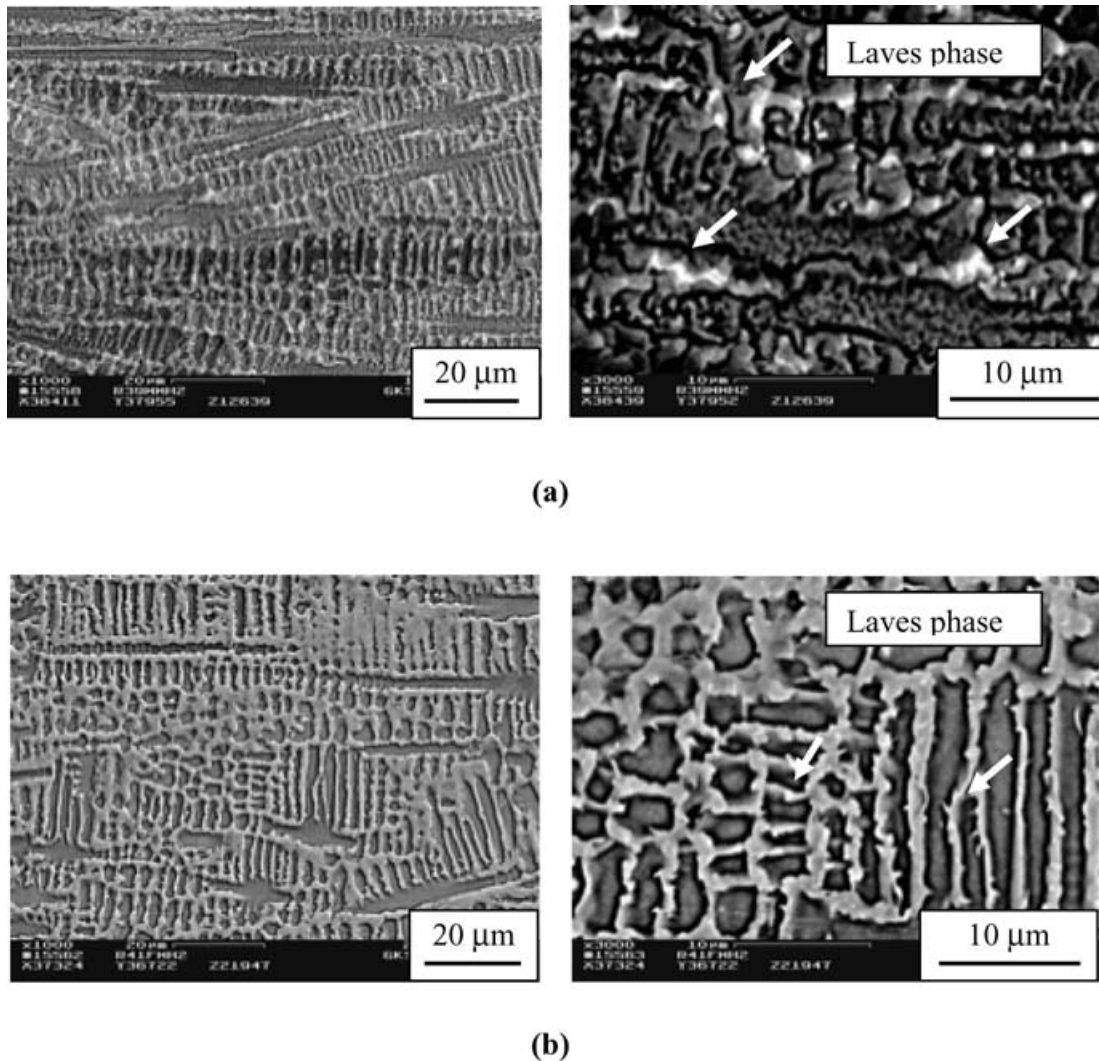
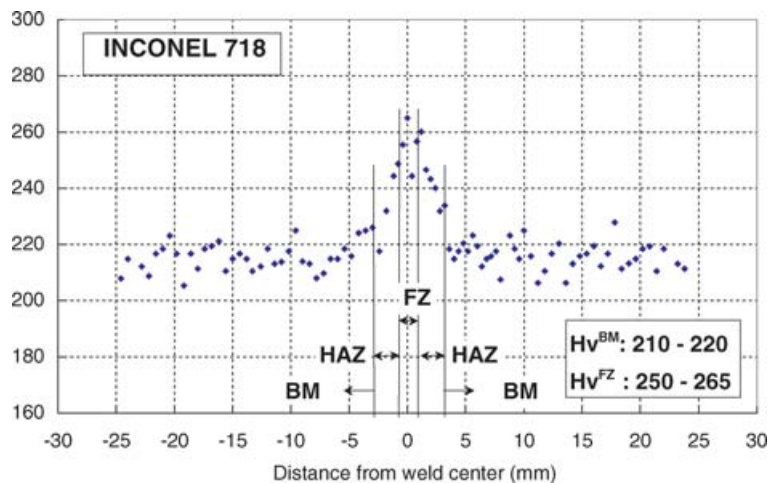
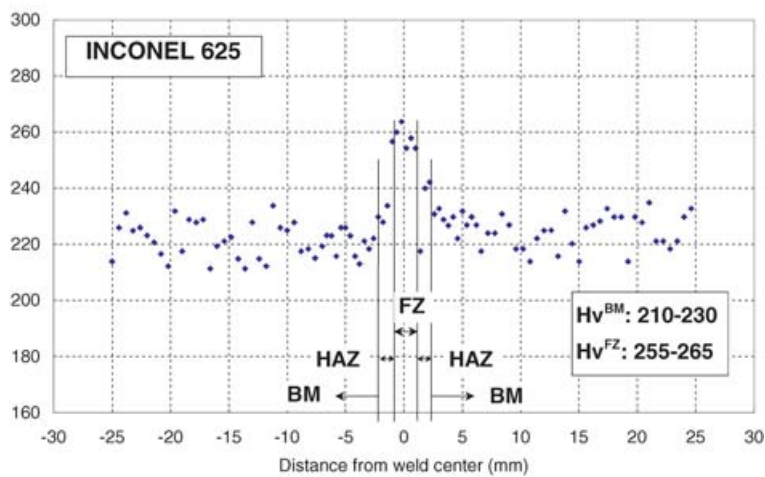


**Fig. 3** SEM microstructures of (a) Inconel 718 fusion zone and its higher magnification, (b) Inconel 625 fusion zone and its higher magnification showing fine discrete Laves particles.



(a)



(b)

Fig. 4 Hardness profiles of LBW superalloys (a) Inconel 718, (b) Inconel 625.

Table 2 Mechanical properties of the BM and LBW for alloys Inconels 718 and 625

Material	Yield strength $R_{p0.2}$ (MPa)	Ultimate tensile strength $R_m$ (MPa)	Total elongation A (%) (gauge length 40 mm)	Joint efficiency in terms of $R_m$ (%)	Joint efficiency in terms of A (%)	Mismatch ratio, $M^a$
Inconel 718 (BM)	469	892	56	–	–	–
Inconel 718 (LBW)	482	853	37.6	96	67.1	1.03
Inconel 625 (BM)	485	854	50.7	–	–	–
Inconel 625 (LBW)	481	858	44	100.5	86.8	0.99

Values are average of three specimens.

<sup>a</sup>  $M = \frac{R_{p0.2LBW}}{R_{p0.2BM}}$  (Ratio of the yield strength of the weld metal to the yield strength of the base metal).

## RESULTS AND DISCUSSION

### Microstructure

Cross sections of both laser-beam weldments are given in Fig. 2. The laser beam welding (LBW) process has pro-

duced rather narrow fusion zones (FZ) with approximately 1 mm width at mid-section, while at the top and root of the weldment the FZ is widened to about  $2H = 2$  mm. A recrystallized microstructure within a very narrow band (adjacent to FZ) is observed in the HAZ of both weldments,

Fig. 2b and d. A very fine structure is detected at the FZ due to the rapid solidification. A detailed microstructural examination concerning the formation of Laves phase has been carried out. SEM micrographs are shown in Fig. 3 for both alloys. In the FZ of Inconel 718, Laves phase is recognizable as bright particles, Fig. 3a. These phases are rich in Nb and Mo, as determined by using EDAX analysis. The FZ of Inconel 625, Fig. 3b, contains also bright

coloured Laves phase, again rich in Mo and Nb as indicative feature of Laves phases. The amount of segregation formation, though, is much less pronounced in both alloys compared to conventional high heat input welding processes where the time period for solidification of the weld pool is longer, because a low heat input and rapid cooling rate of the weld metal is met in laser-beam welding.<sup>6</sup> Similar observation is also being made in this investigation.

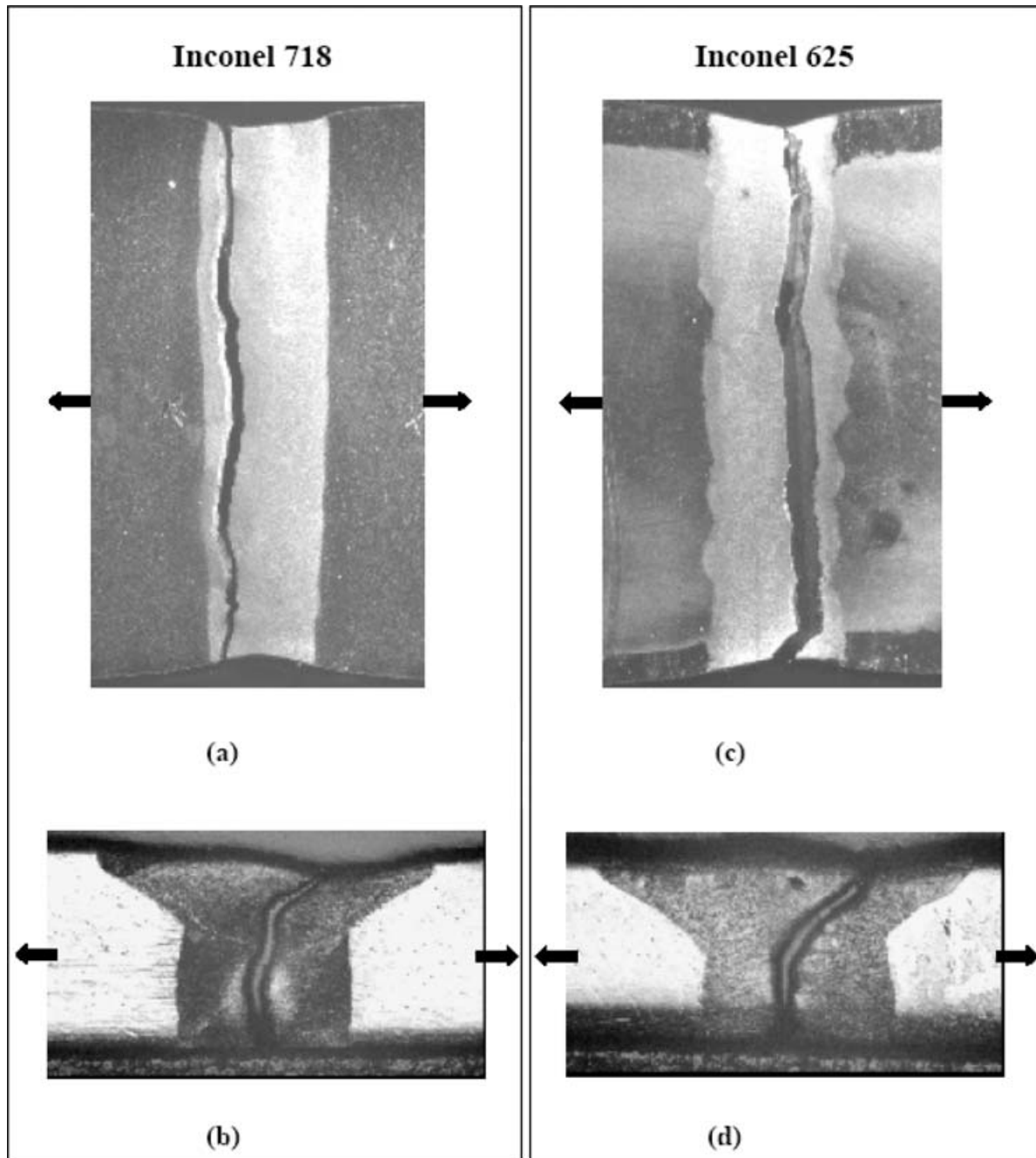


**Fig. 5** Transverse tensile specimens containing welds showing the fracture paths, (a) Inconel 718 along the width and (b) along the thickness, (c) Inconel 625 along the width and (d) along the thickness of the specimen.

### Microhardness

Microhardness measurements ( $HV_{0.2}$ ) have been conducted throughout the BM, HAZ and the FZ for both alloys in order to determine the hardness properties of different regions. For Inconel 718, BM hardness values are around 210–220  $HV_{0.2}$  (Fig. 4a) and it increases at the HAZ and in the FZ to a peak value of 265  $HV_{0.2}$ . The BM hardness of Inconel 625 shows slightly higher scatter than 718 and it has a range of 210–230  $HV_{0.2}$  (Fig. 4b). As in Inconel 718, hardness increases in the FZ to a peak value of 265  $HV_{0.2}$ . It has been reported that the presence of the Laves phase, with high Nb and Mo concentrations, affects the weld metal hardness values.<sup>2,4</sup> In this study, the increase in FZ hardness values can be attributed to the existence of Laves phase containing hard and brittle particles. This increase indicates some degree of strength overmatching (weld yield strength higher than the BM one) nature of the laser-beam weld.

### Room temperature tensile properties

The room temperature tensile properties of the BM and the FZ for both alloys obtained from flat transverse tensile tests are given in Table 2. These transverse flat weld specimens have failed from the FZ as shown in Fig. 5, for both alloys. It can be expected that ductile fracture process via void initiation, growth and coalescence may have taken place with the involvement of hard and brittle Laves particles. However, no detailed fracture surface examination was conducted so far.

The results indicate that LBW joints have comparable yield and ultimate tensile strengths with the BM. The mismatch ratios ( $M$ ) are negligibly small (1.03 and 0.99 for Inconels 718 and 625, respectively). These results can be interpreted as ‘even-matching’. However, the tensile test results show that the ductility has decreased in laser-beam-welded joints compared to the BM in both alloys. The presence of hard and brittle Laves particles within

**Table 3** Results of fracture toughness tests

Material	CTOD $\delta_{5max}$ (mm)		
	BM	FZ	HAZ
Inconel 718	0.89	0.59	0.75
	0.98, 0.74, 0.97, 0.86	0.51, 0.59, 0.79, 0.70, 0.47, 0.60, 0.49	0.60, 0.82, 0.85, 0.77, 0.80, 0.67
Inconel 625	0.87	0.66	0.76
	0.75, 0.93, 0.91, 0.87	0.88, 0.56, 0.78, 0.53, 0.56, 0.62	0.74, 0.71, 0.71, 0.83, 0.73, 0.81

Values are average of minimum four tests.

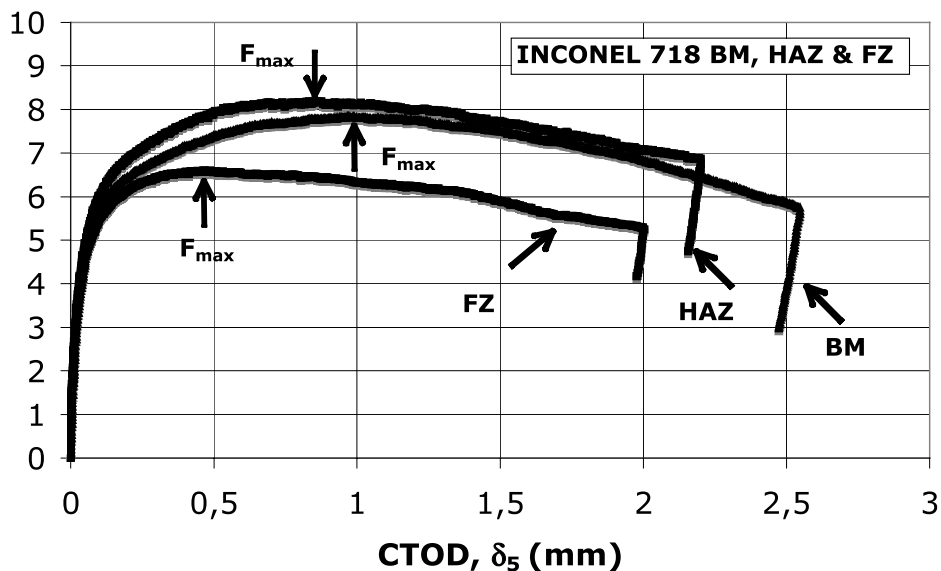


**Fig. 6** Load-CTOD curve of BM, HAZ and FZ regions for Inconel 718 indicating the maximum loads where the fracture toughness values are read.

the FZ promotes the formation of micro-voids either via debonding of particle–matrix interface or particle failure depending on the size and distribution of the particles. This in turn leads to an observed decrease of the ductility of the FZ.

### Fracture toughness and R-curve determination

Fracture toughness tests were carried out at room temperature using 3.2-mm-thick C(T) 50 specimens. Specimens were notched at BM, FZ and HAZ, with  $a/W = 0.5$  and utilized configurations are given in Fig. 1.

CTOD,  $\delta_5$  values (see Fig. 1 for this technique) obtained from the fracture toughness tests are summarized in Table 3. The given values correspond to the maximum load reached during testing. Fracture toughnesses of the BM and HAZ for both materials are similar, whereas the weld region fracture toughness of Inconel 718 is lower compared to 625 as given in Table 3. In both materials, the BM exhibits the highest fracture toughness and weld metal the lowest, at room temperature. As an example, the load-CTOD curves of the three tests of Inconel 718 are given in Fig. 6, obtained from BM-, HAZ- and FZ-notched specimens.

Both materials in all three notch locations, exhibited stable crack growth and no pop-in behaviour has been detected. In Inconel 718, where the pre-crack was located in the FZ, crack almost always deviated towards the interface between the weld and the BM and propagation was partly in the BM. Similarly, when the pre-crack was located at the HAZ in Inconel 718, in all cases, the crack visibly deviated towards the BM, due to the strength overmatching nature of the weld zone. In Inconel 625-FZ notched specimens, crack propagation followed somehow a similar pattern to Inconel 718 FZ specimens where it deviated mostly to the interface, and then propagated in the BM. The crack propagation in Inconel 625 HAZ specimens was also similar to Inconel 718; the crack often deviated towards the BM and propagated in this region. However, for some specimens crack growth was mainly along the interface. In both alloys, the path of the stable crack growth was towards the softer base materials although transverse tensile specimens did not reveal strong strength mismatch as microhardness results have suggested. Typical crack propagation directions for both materials are given in Fig. 7.

The CTOD R-curves for BM, FZ and HAZ regions of Inconel 718 and 625 are shown in Fig. 8. The comparison between the two BM R-curves is shown in Fig. 9 and in Fig. 10a and b the comparison for HAZ and FZ regions is shown for both materials. The maximum load fracture toughness values reported in Table 3 can be seen at the very early stages of the R-curves shown in Fig. 8. Obviously, a significant portion of the R-curves is representing the

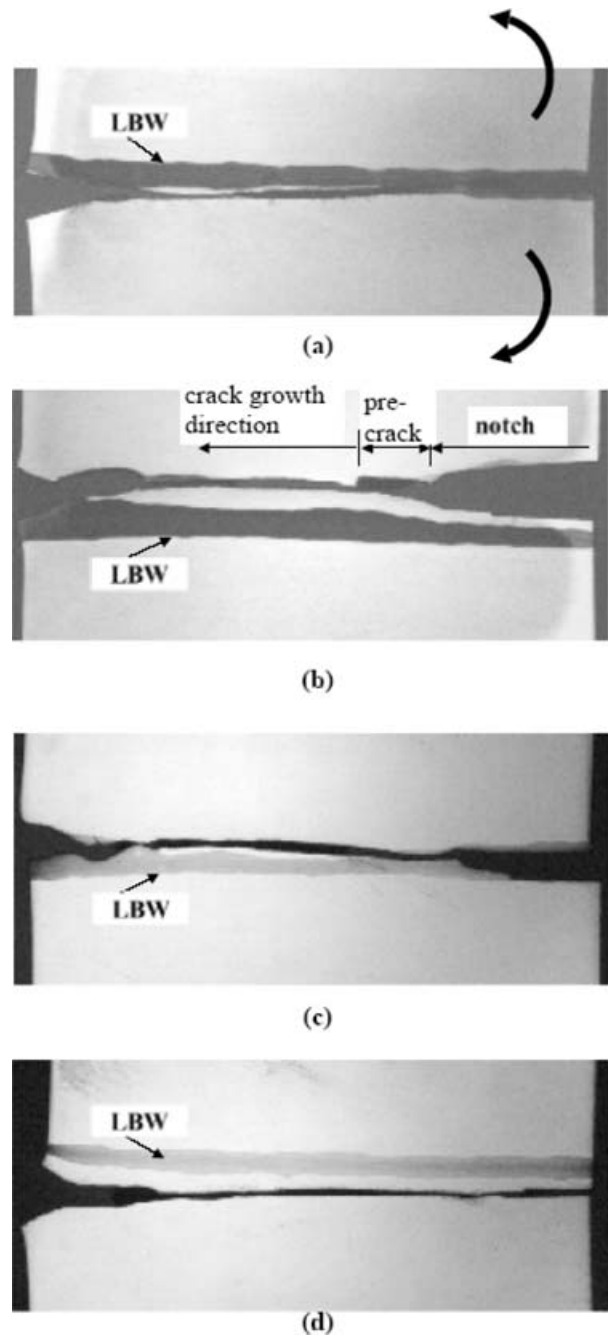
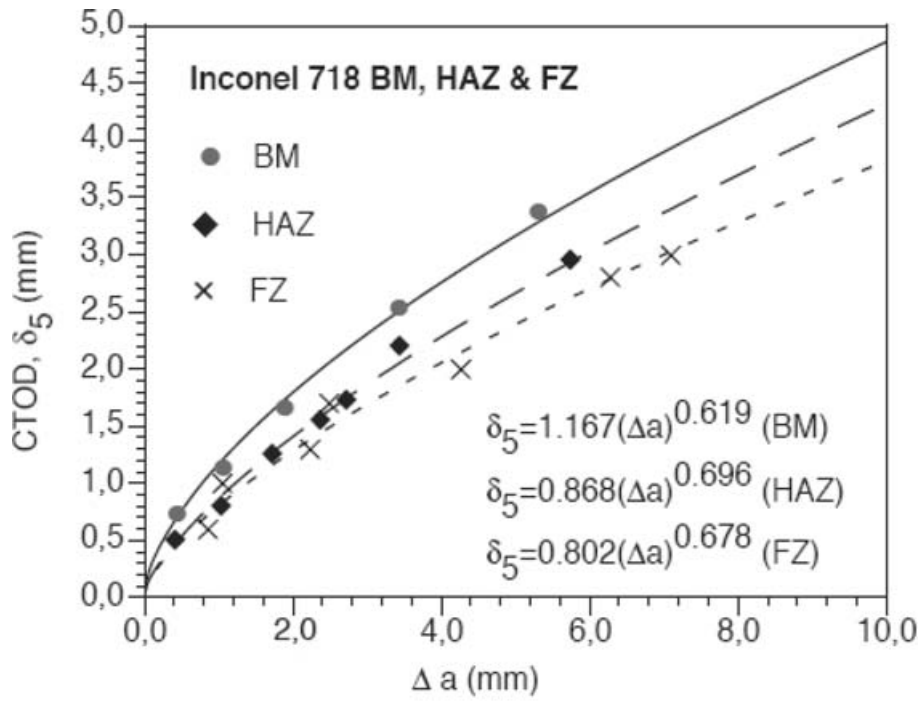
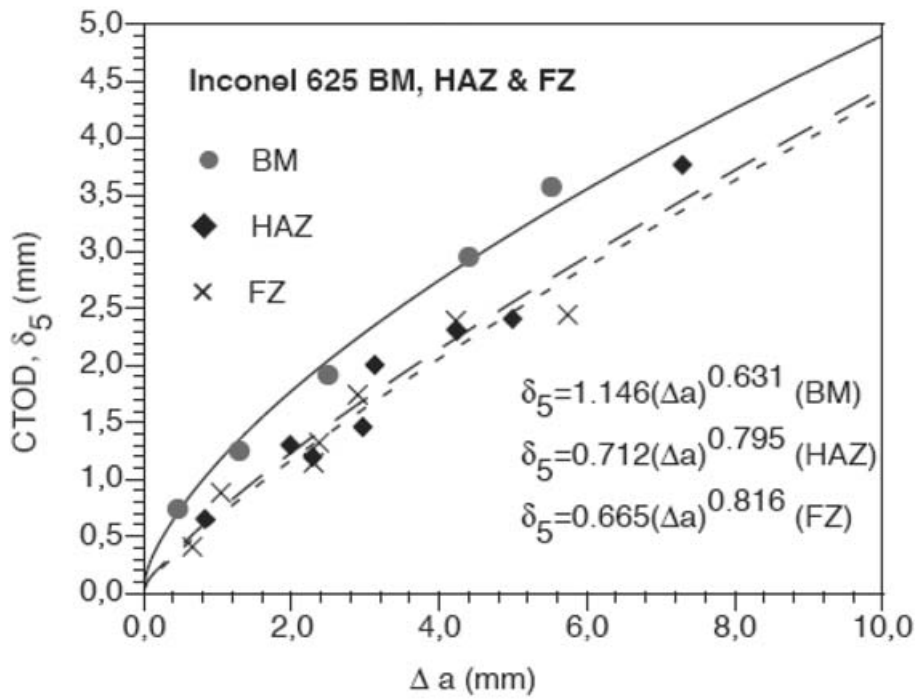


Fig. 7 Crack propagation directions for (a) Inconel 718 FZ, (b) Inconel 718 HAZ, (c) Inconel 625 FZ, (d) Inconel 625 HAZ.

unloading parts of the load-deformation curves as exemplarily shown in Fig. 6. In all CTOD R-curves obtained using multiple specimen technique, the curve fitted description of the resistance curves is given. For both materials, highest R-curves were obtained for the BMs, Fig. 8, compared to the FZ and HAZ R-curves. Similar R-curves for both BMs are shown in Fig. 9. The comparison between FZ and HAZ regions of both materials did not reveal



(a)



(b)

Fig. 8 Crack resistance (R-curve) curves for (a) Inconel 718 BM, HAZ and FZ, (b) Inconel 625 BM, HAZ and FZ.

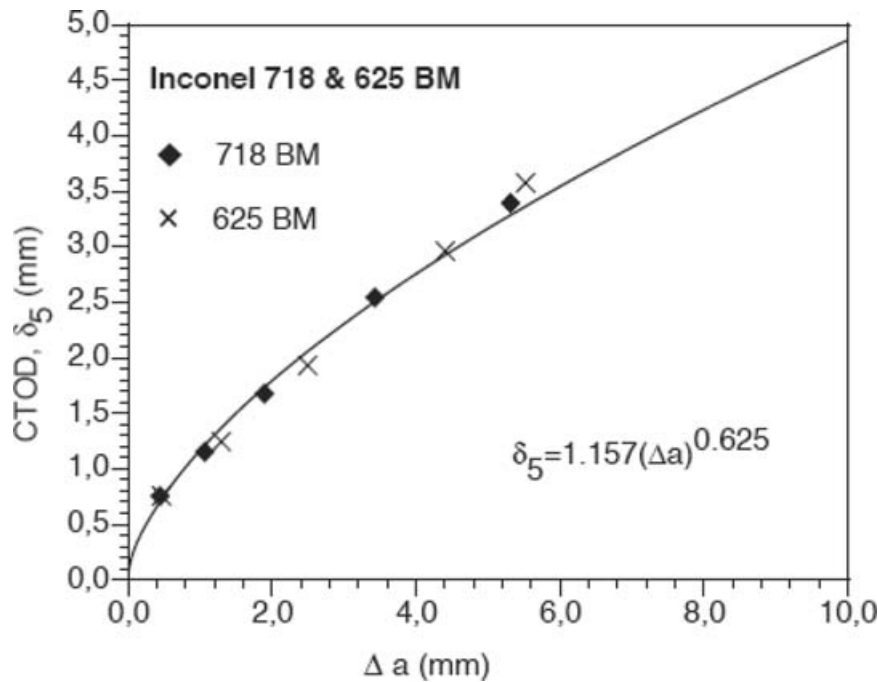


Fig. 9 Comparison of crack resistance R-curves for Inconels 625 and 718 BM.

significant difference as shown in Fig. 10. Therefore, it can be concluded that the RT fracture toughness levels of both materials are similar in BM and laser-beam-welded conditions. The fracture toughness of these materials can be described in the following terms;

$$\delta_5 = 1.157(\Delta a)^{0.625} \quad (\text{BM})$$

$$\delta_5 = 0.726(\Delta a)^{0.740} \quad (\text{FZ})$$

$$\delta_5 = 0.813(\Delta a)^{0.715} \quad (\text{HAZ})$$

By presenting the crack resistance curves in these forms, one can conduct a flow assessment analysis using FITNET Fitness-for-Service Procedure<sup>18</sup> for laser-beam-welded Inconel 718 and 625 structures.

## CONCLUSIONS

The conclusions reached in this investigation are as follows:

- CO<sub>2</sub> laser-beam welding of 3.2-mm-thick Inconel 718 and 625 has produced sound welds in butt-joint configurations.
- Due to the high cooling rates associated with the laser-beam welding process, both joints exhibit fine dendritic solidification microstructures in the FZ, no microfissuring has been observed. Hard and brittle Laves phase has been detected in the FZs of both materials. Hardness increases of about 20% in both weld regions have been observed.

- Joint efficiencies of the weld regions in terms of tensile strength are very good (96% and 100.5%, for Inconels 718 and 625, respectively). LB welding did not cause a decrease in the yield strength of the materials, but there is a slight decrease in the ductility in the weld regions when they are determined by testing of transverse specimens.
- The weld regions exhibit lower CTOD  $\delta_5$  values at maximum loads, while the HAZ fracture toughness lies between the weld region and the BM.
- Similar to the maximum load fracture toughness results, the R-curves of the weld regions were lower than the BMs.

## Acknowledgements

The authors would like to thank Mr. V. Ventzke, GKSS and Ms. S. E. Eren, Munich Technical University, for their contributions in the microstructural examinations and testing programme, respectively.

## REFERENCES

- 1 Thermal and mechanical properties of Inconel 718 and 625. Special Metals Corporation Publication, 2005. [www.specialmetals.com/products](http://www.specialmetals.com/products).
- 2 Ram, G. D. J., Reddy, A. V., Rao, K. P. and Reddy, G. M. (2004). Control of laves phase in Inconel 718 GTA welds with current pulsing. *Sci. Technol. Weld. Joi.* **9**, 390–398.

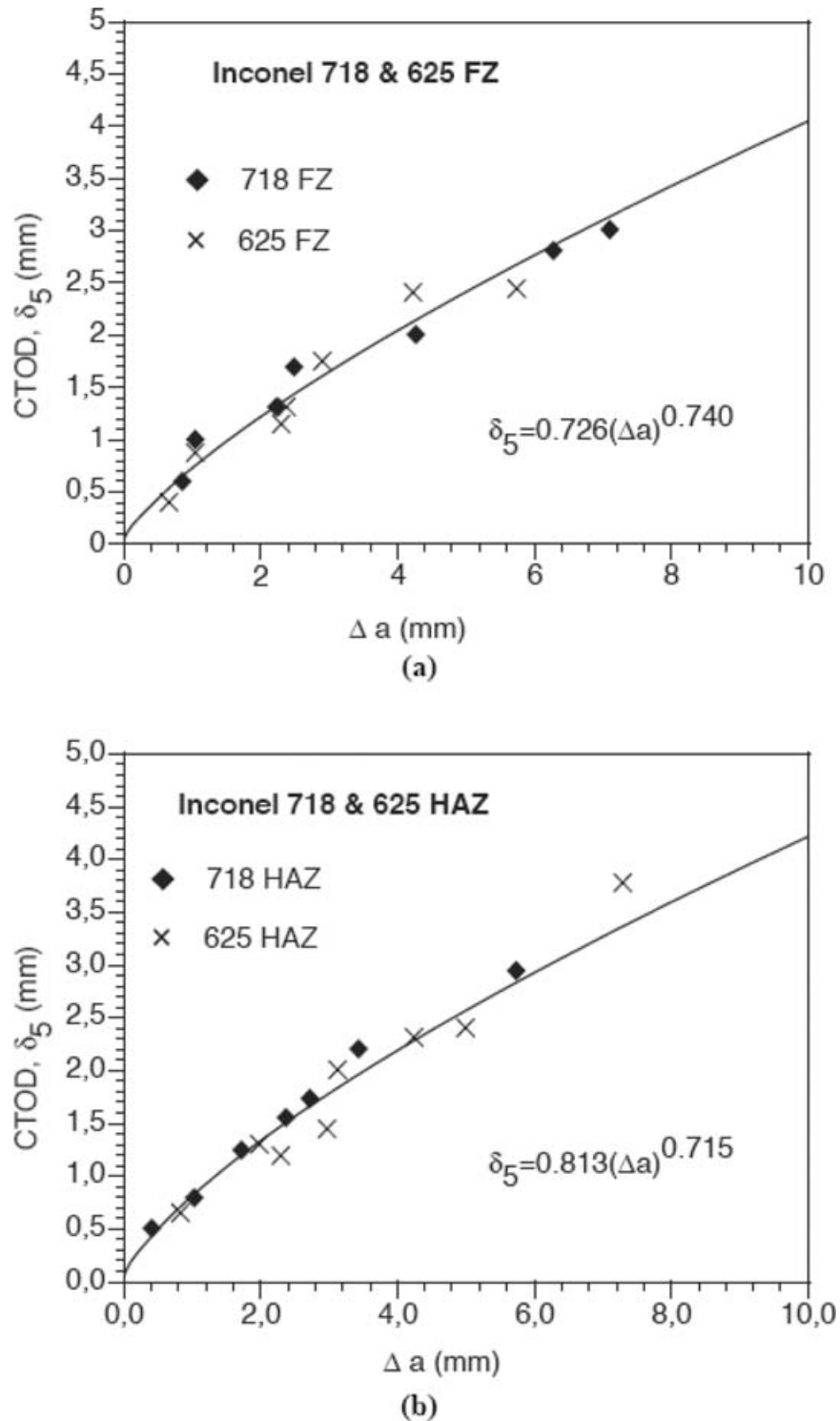


Fig. 10 Comparison of crack resistance R-curves for Inconels 625 and 718 (a) FZ and (b) HAZ.

3 Gregori, A. (2003). *A Survey of Welding and Repairing of Nickel Superalloys for Gas Turbines*. TWI, Report Nr. 774.

4 Ram, G. D. J., Reddy, A. V., Rao, K. P., Reddy, G. M. and Sundar, J. K. S. (2005). Microstructure and tensile properties of

Inconel 718 pulsed Nd-YAG laser welds. *J. Mat. Process. Technol.* **167**: 73–82.

5 Çam, G. and Koçak, M. (1998). Progress in joining of advanced materials. *Int. Mater. Rev.* **43**, 1–44.

- 6 Radhakrishna, C. and Rao, K. P. (1997). The formation and control of laves phase in superalloy 718 welds. *J. Mater. Sci.* **32**, 1977–1984.
- 7 Qian, M. and Lippold, J. C. (2003). Liquation phenomena in the simulated heat affected zone of alloy 718 after multiple postweld heat treatment cycles. *Weld. J.* **6/03**, 145-S–150-S.
- 8 Gobbi, S., Zhang, L., Norris, J., Richter, K. H. and Loreau, J. H. (1996). High powder CO<sub>2</sub> and Nd:YAG laser welding of wrought Inconel 718. *J. Mater. Process. Technol.* **56**, 333–345.
- 9 Gregori, A. and Bertaso, D. (2004). *Welding and Deposition of Nickel Superalloys 718, Waspalloy and Single Crystal Alloy CMSX-10*. TWI, Report Nr. 811.
- 10 Ferro, P. (2003). *Numerical and Experimental Analysis of the Electron Beam Welding of a Nickel Based Superalloy*. Ph. D. Thesis, University of Padova, Spain.
- 11 Çam, G., dos, Santos J. F., Koçak, M., Fischer, A. and Ratjen, R. (1998). *Properties of Laser Beam Welded Superalloys Inconel 625 and 718. ECLAT-European Conference on Laser Treatment of Materials*, 22–23, Germany, pp. 333–338.
- 12 Patterson, R. A. and Milewski, J. O. (1985). GTA weld cracking alloy 625 to 304L. *Weld. J.* **64**, 227s–231s.
- 13 Cieslak, M. J. (1991). The welding and solidification metallurgy of alloy 625. *Weld. J.* **70**, 49s–56s.
- 14 The European Commission funded Brite-Euram Project ASPOW. *Assessment of Quality of Power Beam Welded Joints*. Project Nr. BRPR95-0021.
- 15 Mills, W. J. (1984). Effect of heat treatment on the tensile and fracture toughness behavior of alloy 718 weldments. *Weld. J.* **63**, 237s–245s.
- 16 Mills, W. J. (1989). *Fracture Toughness Variations for Alloy 718 Base Metal and Welds*. In: *Conference on Superalloy 718 - Metallurgy and Applications* (Edited by E. A. Loria). TMS, Warrendale, PA, pp. 517–530.
- 17 ASTM E8-95a, Standard Test Methods for Tension Testing of Metallic Materials, 1995 *Annual Book of ASTM Standards* **03.01**, 56–76.
- 18 FITNET, European Fitness-for-Service Network, Proposal Nr. GTC1-2001-43049, Contract Nr. GIRT-CT-2001-05071, [www.eurofitnet.org](http://www.eurofitnet.org).